Phys Chem Minerals (1985) 12:77–85

PHYSICS AND CHEMISTRY OF MINERALS

Interaction Between Fluorine and Silica in Quenched Melts on the Joins SiO_2-AlF_3 and SiO_2-NaF Determined by Raman Spectroscopy

Bjørn O. Mysen and David Virgo
Geophysical Laboratory, Carnegie Institution of Washington, 2801 Upton Street, Washington, DC 20008, USA

Abstract. The solubility mechanism of fluorine in quenched SiO_2-NaF and SiO_2-AlF_3 melts has been determined with Raman spectroscopy. In the fluorine abundance range of F/(F+Si) from 0.15 to 0.5, a portion of the fluorine is exchanged with bridging oxygen in the silicate network to form Si–F bonds. In individual SiO_4-tetrahedra, one oxygen per silicon is replaced in this manner to form fluorine-bearing silicate complexes in the melt. The proportion of these complexes is nearly linearly correlated with bulk melt F/(F+Si) in the system SiO_2-AlF_3, but its abundance increases at a lower rate and nonlinearly with increasing F/(F+Si) in the system SiO_2-NaF. The process results in the formation of *nonbridging oxygen* (NBO), resulting in stabilization of $Si_2O_5^{2-}$ units as well as metal (Na^+ or Al^{3+}) fluoride complexes in the melts. Sodium fluoride complexes are significantly more stable than those of aluminum fluoride.

Introduction

The transport and thermodynamic properties of fluorine-bearing silicate melts differ significantly from those of their fluorine-free equivalents. It has been shown, for example, that the fluidity and electrical conductivity of silicate melts increase rapidly with increasing fluorine content (Kozakevitch 1954; Hariyama and Camp 1969; Shinozaki et al. 1977). The liquidus temperatures of fluorine-bearing silicate systems are dramatically lowered compared with those of the fluorine-free equivalents. On a molar basis, the magnitude of the freezing-point depression resembles that of water (Wyllie and Tuttle 1961; Kovalenko 1978; Manning 1981; Danckwerth 1981). This observation has led to the suggestion (e.g., Manning 1981) that the solubility mechanisms of water and fluorine in silicate melts may resemble each other.

Observations such as those above have led to the suggestion that solution of fluorine in silicate melts and glasses results in significant depolymerization (a process in which the ratio of nonbridging oxygen per tetrahedral coordinated cations, NBO/*T*, increases). The detailed nature of the fluorine solubility mechanism is, however, not clear. It has been proposed, for example, that fluorine may replace bridging oxygen in the silicate network structure to form a fluorine-bearing silicate tetrahedral network (Rabinovitch 1983). Alternatively, metal-fluorine complexing has been suggested as the principal fluorine solubility mechanism (Kogarko and Kriegman 1973). Available spectroscopic data (e.g., Takusagawa 1980; Yamamoto et al. 1983) are consistent with a fluorine solubility mechanism involving both fluorine substitution for oxygen in the silicate network as well as fluoride complexing associated with metal cations such as Na^+. Aluminum generally is a network former in fluorine-free silicate melts; however, in view of the aluminofluoride complexing observed in melts on the joins AlF_3-NaF, AlF_3-KF and AlF_3-LiF (Gilbert et al. 1975), aluminum fluoride complexes resembling AlF_6^{3-} and AlF_4^- may also exist in fluorine-bearing aluminosilicate melts.

In order to provide a quantitative basis on which to describe the fluorine solubility behavior in aluminosilicate melts, it is necessary to determine (1) the types of fluorine-bearing complexes, (2) the resulting effect of dissolved fluorine on the silicate melt structure and (3) the relative stabilities of these complexes. In the present report, data have been obtained on the roles of NaF and AlF_3 added to SiO_2 melts in order to define the details of the structural roles of these petrologically important, and possibly structurally significant, different components.

Experimental Methods

Compositions studied were along the joins SiO_2-NaF and SiO_2-AlF_3 (Table 1), with the F/(F+Si) ranging from about 0.15 to 0.50. The structural features of quenched melts in the two systems will be compared on the basis of this ratio. The samples (1–2 mm^3 chips of quenched melts) for spectroscopic studies were formed by melting

Table 1. Compositions (wt.%) of quenched melts

	NSF10	NSF5	NSF2	NS5	AFS18	AFS9	AFS6	SA10
SiO_2	87.74	78.16	58.86	82.90	92.30	86.56	81.10	90.00
Al_2O_3	–	–	–	–	–	–	–	10.00
Na_2O	–	–	–	17.10	–	–	–	–
AlF_3	–	–	–	–	7.70	13.44	18.90	–
NaF	12.26	21.84	41.14	–	–	–	–	–
F/(F+Si)	0.167	0.286	0.500	–	0.152	0.250	0.333	–

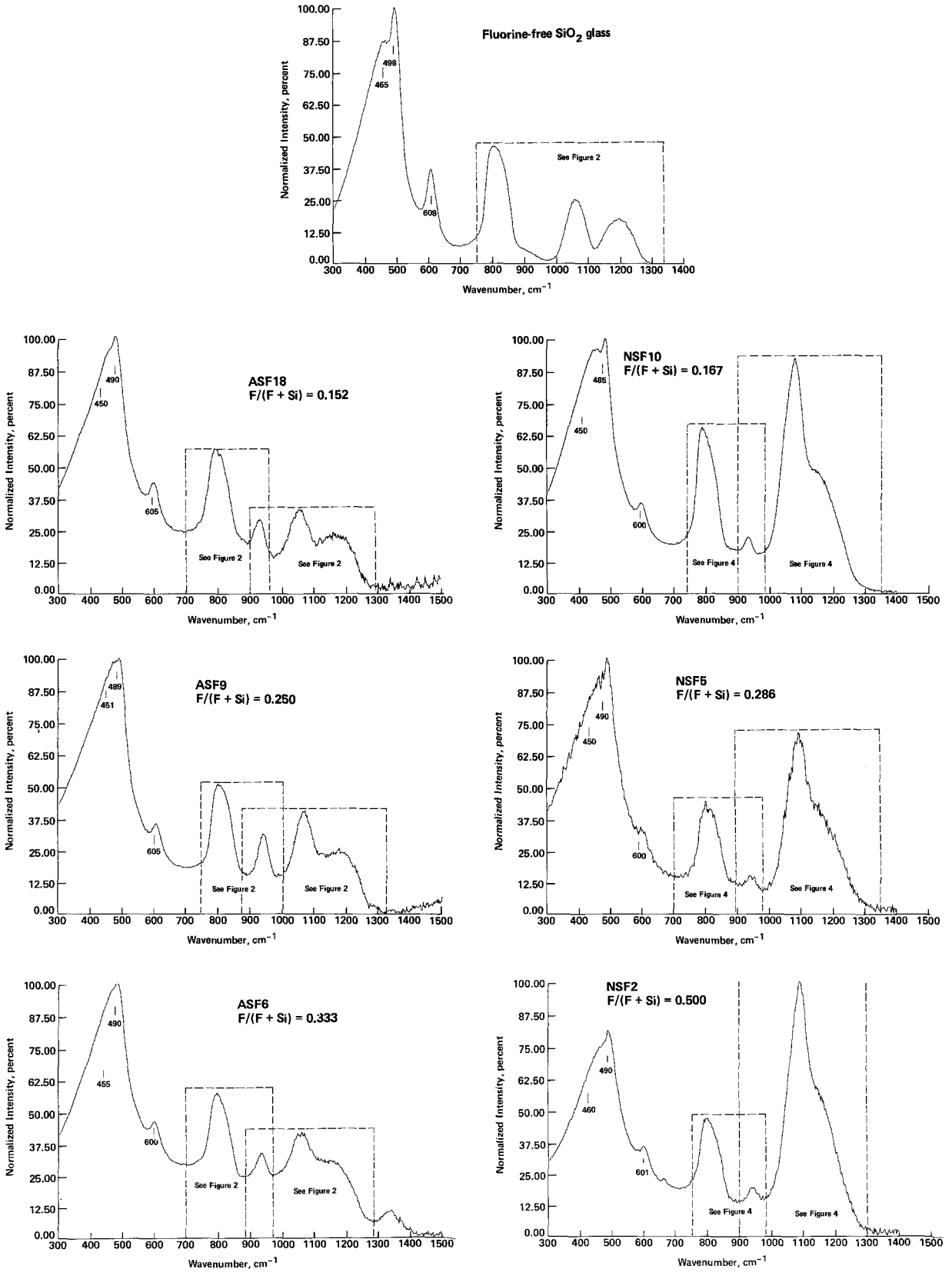

Fig. 1. Temperature- and frequency-corrected, unpolarized Raman spectra of quenched melts on the joins SiO_2-NaF and SiO_2-AlF_3. Dashed boxes indicate portions of spectra selected for statistical curve-fitting, the results of which are shown in Figures 2 and 4

oxide + fluoride mixtures of the desired compositions in sealed Pt containers in 1-atm, vertical, $MoSi_2$-heated quench furnaces. A triple-walled container with 3 mm I.D. and 7 mm O.D. was used. The triple-walled containers were employed in order to ensure that fluorine [whether as fluorine gas (unlikely) or as a fluoride complex (e.g., NaF or SiF_4, perhaps more likely)] was not lost by volatilization (due to the high vapor pressure of fluorine in the systems) during melting. The samples were melted at 1,550° C for 1 hour after heating from 1,000° C to the final temperature at approximately 1° C/min. The samples were quenched in water at a rate of about 500° C/s. Optical examination of the quenched glasses revealed no evidence for phase separation although gas bubbles (air trapped during melting) were evident in the samples with the smallest amount of fluorine added.

Structural information was derived from Raman spectra of the quenched melts with an automated Raman spectrometer system described by Mysen et al. (1982a). The 514-nm line of an Ar^+ ion laser operating at 0.5 W was used for sample excitation. Briefly, this system consists of an LSI 11 minicomputer interfaced with a photon counter and the slit- and wavelength drives of the Raman spectrometer. The spectra were corrected for temperature- and frequency-dependent scattering intensity (e.g., Long 1977) prior to statistical analysis with the expression

$$I_c = I_r\{\nu_o^3[-\exp(-hc/kT)+1]\nu/(\nu_o+\nu)^4\}. \quad (1)$$

In equation (1), I_c and I_r are corrected and raw Raman intensities, respectively. The ν_o and ν are the frequencies of the exciting line and the Raman shift, respectively. The intensities in all reported spectra are normalized to the data point of the greatest absolute intensity. The background was subtracted from the uncorrected spectra by least-squares fitting of a line (typically an exponential curve) through the data points at frequencies greater than those where Raman scattering was observed.

As discussed in detail by Seifert et al. (1982) and Mysen et al. (1982a) the curve-fitting is carried out on a completely statistical basis with the method of minimization of least squares developed and described by Davidon (1966), Fletcher and Powell (1963) and Powell (1964a, b). Upon convergence, the minimum value of χ^2 and maximum randomness in residual distribution are obtained. All line parameters (frequency, half-width and intensity) as well as the number of lines are independent variables in the fitting routine.

Compared with the Raman spectra of crystalline materials, the vibrational modes in amorphous materials can be expected to be broader due to distribution of local geometries and vibrational coupling. As shown elsewhere (e.g., Walrafen 1967; Hartwig 1977; Mysen et al. 1982a; Seifert et al. 1982), the Raman spectra of amorphous materials such as silicate glass are statistically best fitted with bands of Gaussian line-shape. A detailed description of these features of the statistical fitting routine is provided by Seifert et al. (1982) and Mysen et al. (1982a).

Results

Raman Spectra and Their Interpretation

Temperature- and frequency-corrected Raman spectra are shown in Figure 1, and segments of the spectra fitted to

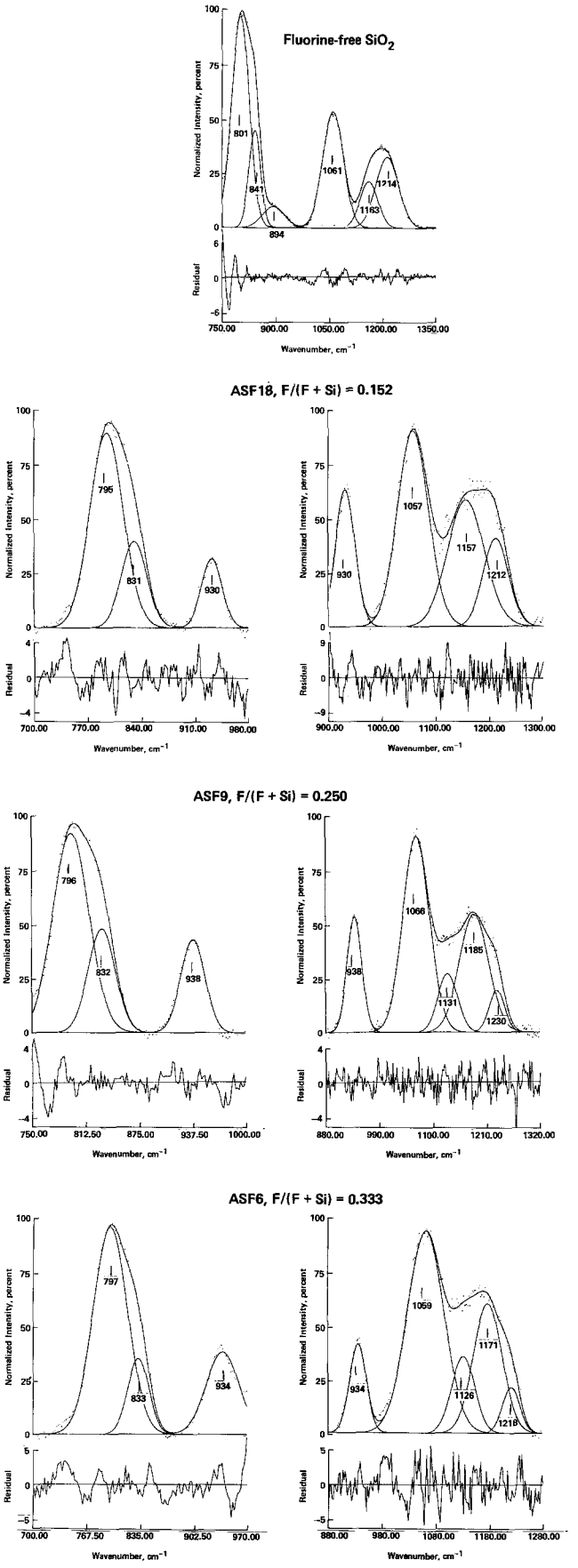

Fig. 2. Statistically-fitted spectra of quenched melts in the system $SiO_2 - AlF_3$ in the frequency regions 700–900 and 850–1,350 cm^{-1}

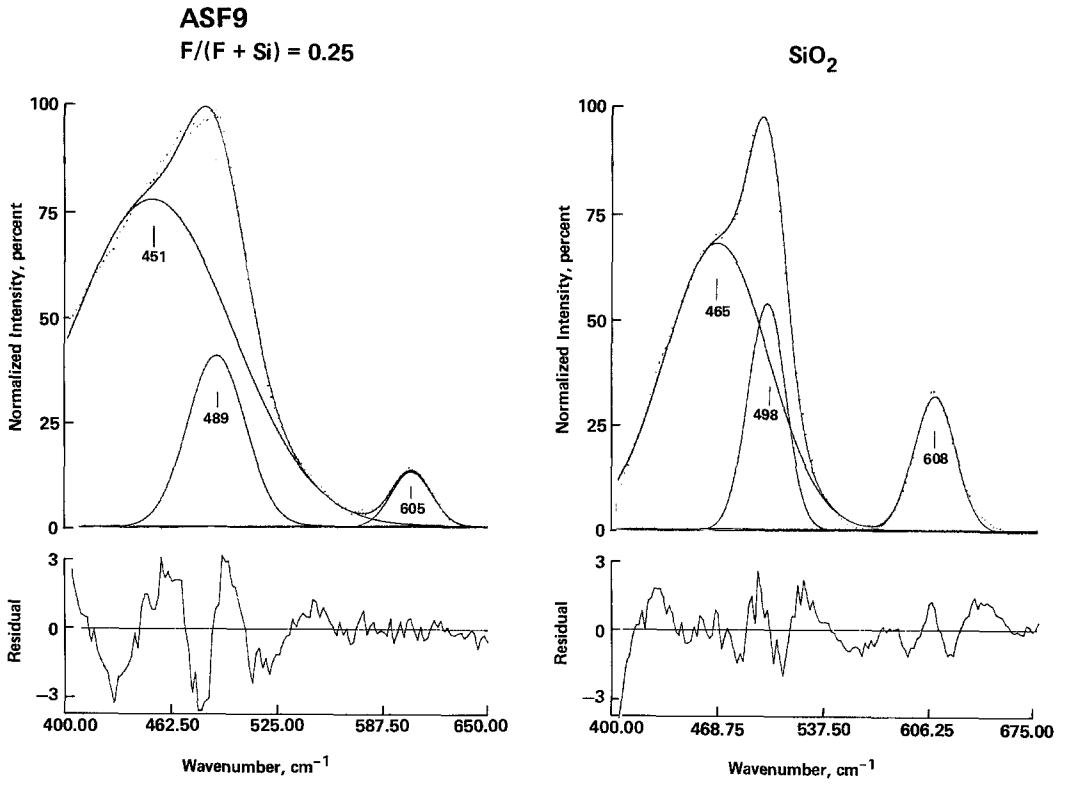

Fig. 3. Examples of statistically-fitted spectra of quenched melts in the system SiO_2-AlF_3 in the low-frequency region (400–675 cm^{-1})

Gaussian curves are shown in Figures 2–4. The spectra of all fluorine-bearing quenched melts retain most of the features of the topology of the spectrum of vitreous SiO_2. These are the broad, asymmetric band near 450 cm^{-1}, the sharp bands near 480 and 600 cm^{-1} (Fig. 3), the asymmetric envelope near 800 cm^{-1} (which probably contains two distinct bands), and two bands centered near 1,160 and 1,210 cm^{-1} (Figs. 2 and 4). A rigorous correlation between the structure and spectra of amorphous SiO_2 still awaits a better understanding of the interatomic bonding. The spectra features can, however, be understood qualitatively in terms of vibrations of interconnected SiO_4^{4-} groups in a three-dimensional network. This network may be described in terms of at least two distinct distributions of Si–O–Si angles (Seifert et al. 1983; Phillips 1984).

In the spectra of quenched melts in the system SiO_2-AlF_3, essentially only one feature differs from the spectrum of vitreous SiO_2. A distinct, sharp band occurs near 935 cm^{-1}. In the deconvoluted spectra (Fig. 3), it is apparent that in the low-frequency region (300–700 cm^{-1}) the same fitted bands result from the deconvolution of this spectral region (450, 480 and 600 cm^{-1}) of all quenched melts along the join SiO_2-AlF_3. In the high-frequency portion (700–1,350 cm^{-1}), the two bands in the broad, asymmetric 800-cm^{-1} region of the SiO_2 spectrum remain in the presence of AlF_3. The 935-cm^{-1} band (Fig. 1) is fitted to a single, symmetric Gaussian line centered between 935 and 940 cm^{-1} for all spectra of quenched melts with different fluorine contents (Fig. 2). In addition to the ~1,060-, ~1,140- and ~1,210-cm^{-1} bands resulting from the presence of three-dimensionally interconnected SiO_4^{4-} tetrahedra in both SiO_2 and SiO_2-AlF_3 quenched melts, increasing fluorine contents in SiO_2-AlF_3 result in a new band near 1,130 cm^{-1}. The topology of this portion of the spectrum resembles that of the high-frequency envelope of Raman spectra of quenched melts in the system $Na_2O-Al_2O_3-SiO_2$ with Na/Al<1 (Fig. 5) where the relative intensity of the 1,130 cm^{-1} increases with increasing Al/Na at constant total Al^{3+} content (Mysen et al. 1980). This intensity increase seems correlated, therefore, with the increased abundance of Al^{3+} without Na^+ for electrical charge-balance.

The spectra of quenched melts in the system SiO_2-NaF as a function of F/(F+Si) resemble those in the system SiO_2-AlF_3. The same new bands occur near 935 and 1,100 cm^{-1} (Figs. 1 and 4), although the exact frequency of the band fitted near 1,130 cm^{-1} in the aluminofluoride-bearing silica samples is slightly lower (1,095 cm^{-1}). The effect of increasing Na/Si on the spectra of melt on the join SiO_2-Na_2O strongly resembles the influence of increasing Na/Si [and, therefore, increasing F/(F+Si)] on the spectra of quenched melts on the join SiO_2-NaF (Fig. 6; see also Mysen et al. 1982b; Furukawa et al. 1981; Matson et al. 1983, for spectroscopic data on melts on the join Na_2O-SiO_2). Similar qualitative observations have been made in infrared spectra of fluorine-bearing quenched alkali silicate glasses (Takusagawa 1980).

The spectra of all samples show the characteristic sharp (20–25 cm^{-1} half-width at half-height) 935-cm^{-1} band, most probably due to Si–F stretch vibrations in melt complexes with one F and three O per Si (e.g., Yamamoto et al. 1983; Dumas et al. 1982; Takusagawa 1980). Yamamoto et al. (1983) calculated and measured the frequency of Si–F stretching as a function of F/(F+O) in the fluorinated silicate tetrahedra in fluorine-doped silica. They found a systematic frequency decrease of about 50 cm^{-1} per bridging oxygen replaced by fluorine, with the 935-cm^{-1} band due to fluorine in the form of a complex with one

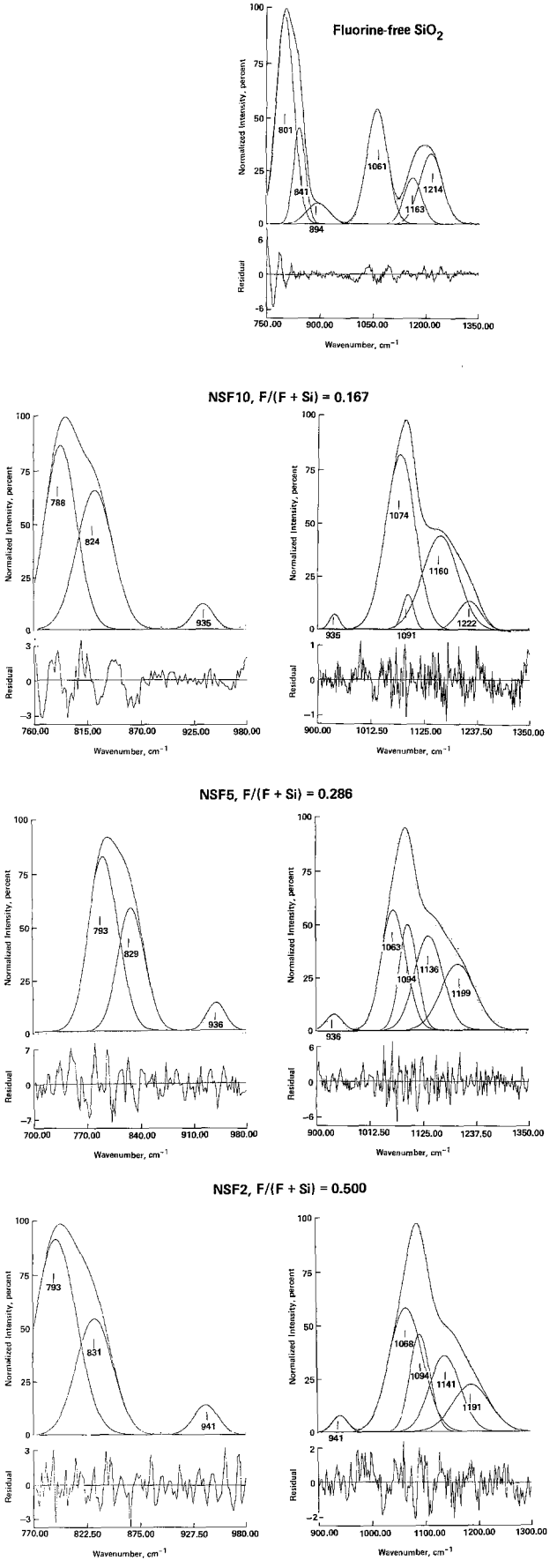

Fig. 4. Same as Figure 2, but for quenched melts in the system SiO_2-NaF

oxygen per silicon replaced by fluorine [F/(F+O)=0.25]. Only the 935-cm^{-1} band is observed in the spectra reported here (Figs. 1, 2 and 4), and it is concluded that whether fluorine is added to the SiO_2 composition as NaF or AlF_3, a significant proportion of the fluorine interacts with the silicate network. In this interaction, only one bridging oxygen per tetrahedron is replaced by fluorine. It is suggested that if fluorine substituted for bridging oxygen in silicate complexes that locally also contain nonbridging oxygen, the frequency of the Si–F stretch vibrations might decrease as systematic functions of the number of nonbridging oxygens per silicon (NBO/Si) in the fluorinated complex. There is no evidence for such features in the Raman spectra. Thus, we suggest that all the oxygens in the fluorine-bearing silicate complexes are bridging.

It is notable that the broad range of Raman bands between 300 and 700 cm^{-1} characteristic of vibrations in AlF_6^{3-} or AlF_4^- complexes, observed, for example, in molten cryolite (Gilbert et al. 1975) cannot be detected in the spectra reported here. Thus, it appears that most, if not all, of the fluorine added as AlF_3 has replaced bridging oxygen in the network of three-dimensionally interconnected SiO_4^{4-} tetrahedra to form Si–F bonds. An electrically neutral complex with one oxygen replaced by fluorine is $Si_2O_3F_2$. Structurally, it may be hypothesized that this complex is envisioned as a double chain terminated on both sides with fluorine:

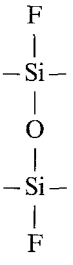

The double-chain will, however, contain nonbridging oxygen the presence of which is considered unlikely (although not ruled out from the spectral data). One cannot exclude from the Raman data structural units with a smaller average number of fluorines per silicon such as, for example, in its simplest form, the $Si_4O_7F_2$ complex:

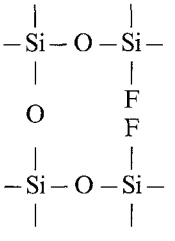

This latter is the simplest fluorine-bearing, three-dimensionally interconnected silicate structure where all oxygens are bridging. In view of the fact that we suspect that the frequencies of Si–F stretch vibrations decrease with increasing NBO/Si of the complex and no such features were observed, we suggest that the fluorinated silicate complexes are three-dimensionally interconnected with some of the bridging oxygens replaced by fluorine (second model above). The $Si_4O_7F_2$ notation is used here. This notation describes the stoichiometry of the simplest three-dimensionally interconnected, fluorine-bearing silicate complex in which only one bridging oxygen is replaced by fluorine in

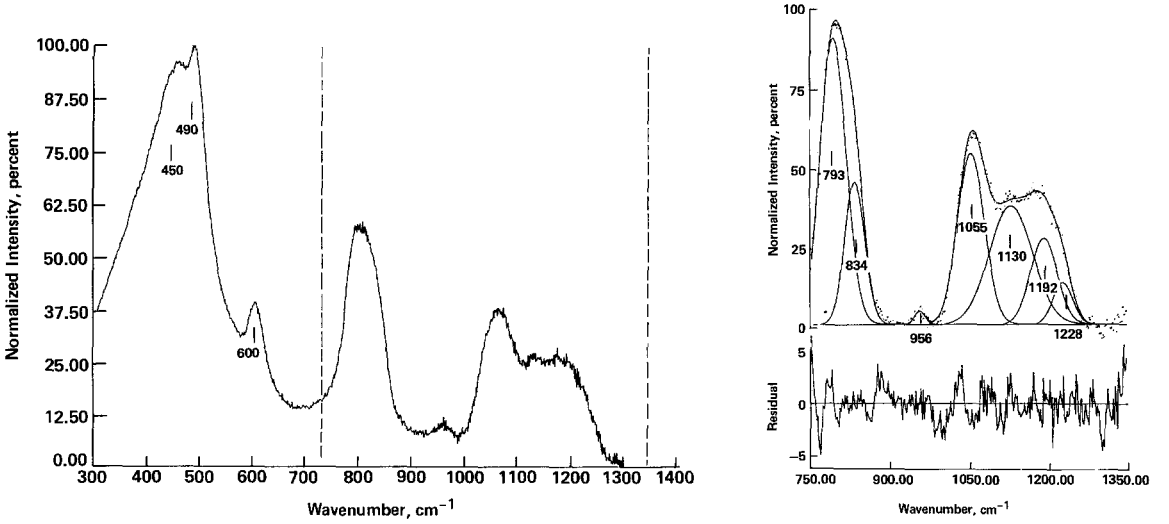

Fig. 5. Temperature- and frequency-corrected Raman spectrum, together with deconvolution in the 750–1,350 cm^{-1} region, of quenched AS10 melt (90 wt.% SiO_2, 10 wt.% Al_2O_3)

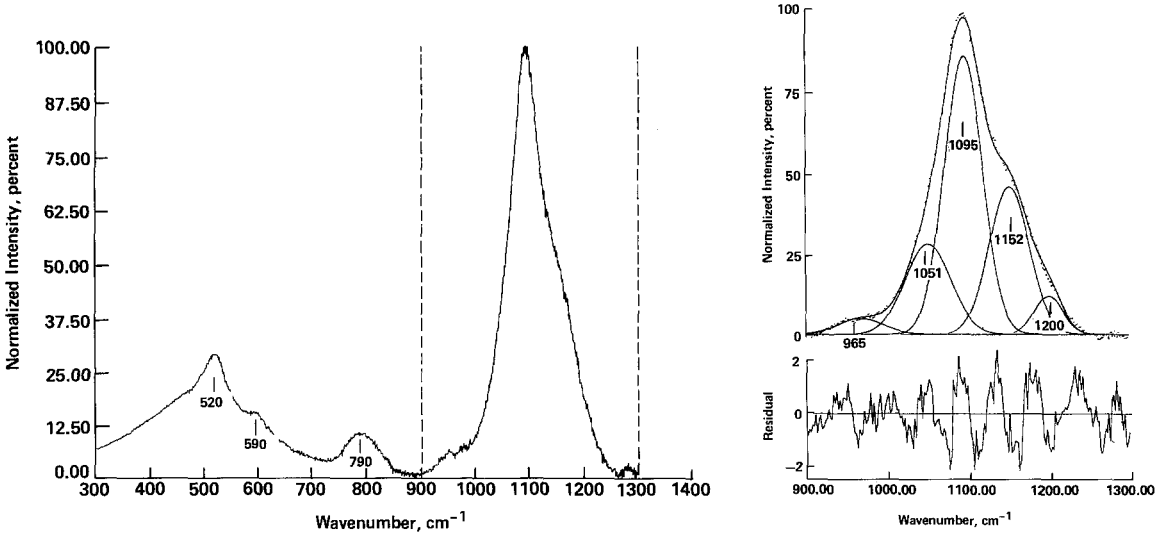

Fig. 6. Temperature- and frequency-corrected Raman spectrum, together with deconvolution in the 900–1,300 cm^{-1} region, of quenched NS5 melt (17.10 wt.% Na_2O, 82.90 wt.% SiO_2)

some of the tetrahedra. The spectra do not preclude the existence, however, of complexes with, on the average, a smaller value of F/O than suggested by the notation $Si_4O_7F_2$. The expressions below are, however, equally valid regardless of which stoichiometry is chosen.

One may, though, suggest that perhaps silicate melt structures cannot be described in terms of relatively simple, distinct structural units. The data presented here cannot be used to distinguish between simple discrete structural units and long-range structural units that locally may exhibit significantly different proportions of non-bridging oxygens, for example. This possibility can, however, be discussed with the aid of published Raman data on quenched melts in $MO-SiO_2$ and M_2O-SiO_2 (*M:* divalent and monovalent metal cation) systems (Brawer and White 1975; Furukawa et al. 1981; Mysen et al. 1982b). Those data (see, in particular Figure 10 in Mysen et al. 1982b) have led to the following conclusions. (1) Those spectra show the existence of only a limited number of $Si-O^-$ stretch bands as a function of M/Si of the melts. The frequencies of each of these types of vibrations are distinctly different and increase in systematic fashion with NBO/Si of the individual structural unit; NBO/Si = 4 with $Si-O^-$ stretch near 850–860 cm^{-1}, NBO/Si = 3 with $Si-O^-$ stretch near 900 cm^{-1}, NBO/Si = 2 with $Si-O^-$ stretch near 950–970 cm^{-1} and NBO/Si = 1 with Si/O^- stretch between 1,095 and 1,130 cm^{-1}. (2) For a specific metal cation (e.g., Na^+), the frequencies of the individual bands are *independent* (within about 5 cm^{-1}) of the bulk melt M/Si, but increase by 20–30 cm^{-1} at constant bulk melt M/Si as the Z/r^2 of the M-cations increases (e.g., $Na^+ < Ca^{2+} < Mg^{2+} < Al^{3+}$). The bands also tend to become somewhat broader. Thus, there is no evidence in the Raman spectra of quenched melts along these joins of a gradual change of polymerization of individual units (or complexes) as the bulk melt polymerization (or M/Si) is altered. (3) The relative intensities of the individual $Si-O^-$ stretch bands (which can be converted to relative abundance; Seifert et al. 1981) are systematic functions of bulk melt M/Si. For example, for a given M-cation, the 850 cm^{-1} band intensity decreases as M/Si is lowered from that of an orthosilicate stoichiometry. The 950–970 cm^{-1} band intensity increases

to a maximum at M/Si near that of metasilicate and then decreases with an additional M/Si decrease. The 1,100 cm^{-1} band intensity increases in the M/Si range between meta- and disilicate bulk melt stoichiometry, and then decreases at M/Si less than that of disilicate. (4) These systematic intensity relations (see Figure 10; Mysen et al. 1982b) would not be observed if the $Si-O^-$ stretch vibrations resulted from the existence of the relevant structural units simply as "end-units" of other, less polymerized units (e.g., units with NBO/Si near 2 along edges of larger units with NBO/Si = 1, and units with NBO/Si = 3 in larger units with NBO/Si = 2). As the proportion of NBO/Si = 1 units increased, one would expect a concomitant increase in the intensity of the $Si-O^-$ stretch band intensity from units with NBO/Si near 2. Similarly, the 900 cm^{-1} band intensity would be expected to be positively correlated with that of the 950–970 cm^{-1} bands. Both the early intensity data of Brawer and White (1975) and more detailed recent data by Furukawa et al. (1981) and Mysen et al. (1982b) are inconsistent with such trends.

We conclude, as did Mysen et al. (1980, 1982b) and Furukawa et al. (1981) that distinct structural units are present in the silicate melts. Although the detailed geometries of these units cannot be ascertained, they can be expressed with the stoichiometric expressions SiO_4^{4-}, $Si_2O_7^{6-}$, SiO_3^{2-}, $Si_2O_5^{2-}$ and SiO_2. These entities should be considered as discrete structural units in the silicate melts. In order to maintain local electrical neutrality, these units require association with network-modifying cations (Na^+, K^+, Ca^{2+}, Mg^{2+} and under certain circumstances Al^{3+} etc.). In the absence of evidence to the contrary, we suggest that the fluorine-containing structural units in the melts (whether as fluorinated silicate units or as F^- in association with metal cations such as Na^+ or Al^{3+}) exhibit similar structural behavior in silicate melts.

In analogy with the interpretation of Raman spectra of quenched melts on the joins SiO_2-Na_2O and $SiO_2-Al_2O_3$, the appearance of the band between 1,100 and 1,130 cm^{-1} (depending on whether the metal cation is Na^+ or Al^{3+}) is ascribed to the presence of $Si-O^-$ bonds, most probably in interconnected SiO_4^{4-} tetrahedra with one nonbridging oxygen per silicon (e.g., $Si_2O_5^{2-}$) (e.g., Brawer and White 1975; Furukawa et al. 1981; Mysen et al. 1980, 1982b). The significant broadness of the 1,130-cm^{-1} band (~40 cm^{-1}) in the aluminous quenched melts compared with the sharper ~1,100-cm^{-1} band (half-width ~30 cm^{-1}) in the sodic melts probably results from greater distortion of this structural unit in the aluminous samples.

Raman Band Intensities and Relative Abundance of Structural Units

Qualitatively, the intensity ratios of bands obtained from the fitted spectra (Table 2) indicate that aside from the formation of $Si_2O_5^{2-}$ structural units, the relative proportions of the three-dimensional SiO_2 network units remaining in the fluorine-bearing silica melts have been altered.

The intensity of the 935-cm^{-1} bands may be used as a measure of the concentration of fluorinated silicate complexes (denoted $Si_4O_7F_2$ in this discussion). From the deconvoluted spectra (Figs. 2 and 4), the intensity of this band, normalized to total area of the two bands near 800 cm^{-1} (Table 2) is nearly linearly correlated with the F/(F + Si) of the SiO_2-AlF_3 melts (Fig. 7). Notably, this

Table 2. Intensity ratios (area) from Raman spectra

	$A(935)/A(800)$[a]	$A(1,100)/A_1$[a]	$A(1,160)/A_2$[a]
SiO_2	–	–	0.66
NS5	–	0.60	0.61
SA10	–	0.62	0.26
NSF10	0.05	0.09	0.17
NSF5	0.06	0.30	0.43
NSF2	0.06	0.32	0.43
ASF18	0.16	n.d.[b]	0.32
ASF9	0.23	0.22	0.16
ASF6	0.31	0.22	0.18

[a] $A(800)$, area of (790+830)-cm^{-1} bands; A_1, area of (1,100+1,160+1,210)-cm^{-1} bands; A_2, area of (1,160+1,210)-cm^{-1} bands

[b] Not detected

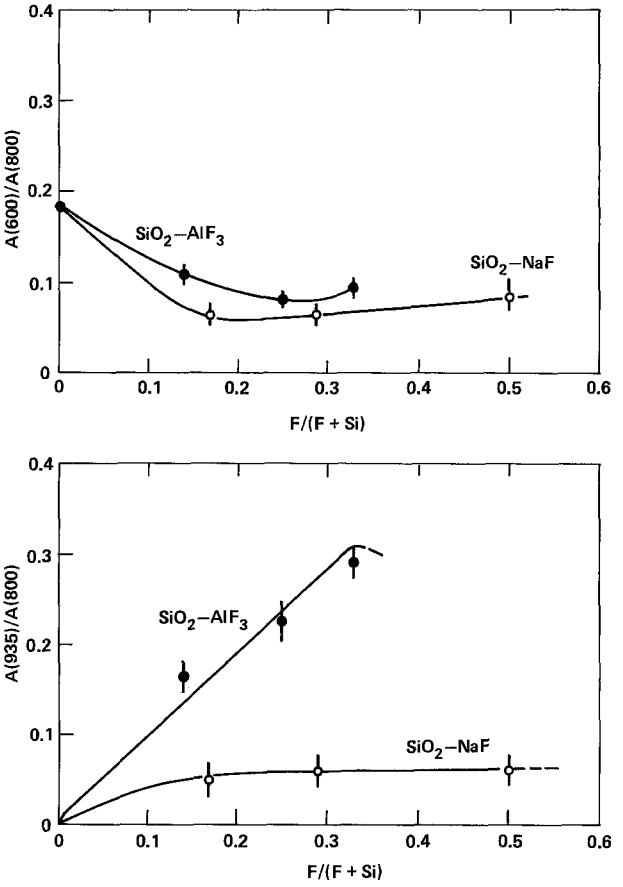

Fig. 7. Intensities of Si–F stretch band (935 cm^{-1}) and Si–O broken bond defect band (600 cm^{-1}) relative to the intensity of (800+830)-cm^{-1} bands (denoted 800 for simplicity) of quenched melts in the systems SiO_2-NaF and SiO_2-AlF_3

line can be extrapolated through the origin. This observation lends support to the suggestion that the principal fluorine-bearing structural unit in the quenched SiO_2-AlF_3 melts may be expressed as $Si_4O_7F_2$. This behavior differs, however, from that of the 935-cm^{-1} band in SiO_2-NaF melts, where the intensity is relatively insensitive to the bulk melt F/(F + Si) (Fig. 7). Its intensity is also significantly less than in the aluminous samples. It is also noted that the intensity of the ~1,100-cm^{-1} band in both series of spectra

increases, and that of the (1,160+1,210)-cm^{-1} band decreases with increasing F/(F+Si) (Table 2).

The intensity data may be used to calculate the proportions of $Si_4O_7F_2$, SiO_2, $Si_2O_5^{2-}$ and metal fluoride units in the melts. The intensity relations in Figure 7 for SiO_2-AlF_3 quenched melts have been used to calibrate the abundance of $Si_4O_7F_2$ as a function of F/(F+Si). The data in this figure can be used for this purpose because the intensity of the 935-cm^{-1} band is linearly correlated with F/(F+Si) of the melt, where this straight line passes through the origin within experimental uncertainty. From this calculation it is evident that in quenched SiO_2-NaF melts more fluorine is dissolved in the melt than can be accounted for in the $Si_4O_7F_2$ or any other fluorine-bearing silicate unit with F/(F+Si)<0.25 (one fluorine per silicon). The remaining fluorine could occur as F^--bearing complexes with Na^+ in close spatial association for electrical balance. The proportion of these complexes can be estimated by mass balance of the total fluorine content of the system. For the spectra of Na-bearing quenched melts, the relative intensity of the 1,100-cm^{-1} band was converted to relative proportion with the aid of the method described by Seifert et al. (1981). Because the only fluorine-free silicate units are SiO_2 and $Si_2O_5^{2-}$, the proportion of SiO_2 is obtained by difference. For the SiO_2-AlF_3 melts if it is assumed that all fluorine resides in fluorine-substituted silica tetrahedra (e.g., $Si_4O_7F_2$), the Al^{3+} added to the melt acts as a network modifier and is associated with $Si_2O_5^{2-}$ structural units. These units may be balanced, for stoichiometric purposes, as $Al_2(Si_2O_5)_3$. In quenched $NaF-SiO_2$ melts, these units are balanced as $Na_2Si_2O_5$. These balanced expressions are not meant to imply that complexes such as $Na_2Si_2O_5$ and $Al_2(Si_2O_5)_3$ exist in the melts as in a crystal structure. Rather, the anionic silicate units and Na^+ and Al^{3+}, respectively, must be closely associated in the melts in order to maintain electric neutrality. This latter assumption is additionally justified in the system SiO_2-AlF_3 because the spectra do not exhibit Al(IV)–O stretch bands (between 750 and 900 cm^{-1}; McMillan et al. 1982; Seifert et al. 1982) that would indicate the presence of aluminate or aluminum-bearing silicate units. The latter structural feature would lead to a systematic frequency decrease of the high-frequency Si–O stretch bands as a function of increasing Al/(Al+Si) (McMillan et al. 1982; Seifert et al. 1982). Such spectral features were not observed (Fig. 2). With this assumption the proportion of $Si_2O_5^{2-}$ can be calculated from mass balance of Al/(Al+Si). The resulting proportions of structural units as a function of F/(F+Si) are shown in Table 3. As is also evident from the raw intensity data in Figure 7, the proportion of $Si_4O_7F_2$ complexes increases at a significantly greater rate with increasing F/(F+Si) in the SiO_2-AlF_3 quenched melts compared with the SiO_2-NaF quenched melts. The rate of change in the proportions of silicate units (relative to fluorine+fluorine-free structural units) shows only small differences between the two systems.

Solubility Mechanisms of Fluorine

The solubility mechanisms of fluorine in SiO_2-NaF and SiO_2-AlF_3 quenched melts can be ascertained from the above data and expressed with the following equations:

$$6SiO_2+2NaF=Si_4O_7F_2+Na_2Si_2O_5 \quad (2)$$

Table 3. Proportions (mole fraction) of coexisting units in melts

	X_{SiO_2}	$X_{Si_2O_5^{2-}}$	$X_{Si_4O_7F_2}$	X_{NaF}	Equilibrium constant (K_1)
SiO_2	1.00	0.00	0.00	0.00	–
NS5	0.67	0.33[a]	0.00	0.00	–
SA10	0.60	0.40[b]	0.00	0.00	–
NSF10	0.78	0.04	0.16	0.02	73
NSF5	0.57	0.14	0.18	0.11	61
NSF2	0.38	0.12	0.21	0.29	71
ASF18	0.85	0.04[c]	0.11	–	–
ASF9	0.76	0.06	0.18	–	–
ASF6	0.43	0.14	0.43	–	–

[a] From Mysen et al. (1982b). The value includes SiO_3^{2-} units ($X_{SiO_3^{2-}}=0.075$; $X_{Si_2O_5^{2-}}=0.255$)

[b] The spectrum (Fig. 3) indicates a very small proportion of SiO_3^{2-} (<1 mole%), which is ignored in the calculations

[c] Not observed in the spectrum (Fig. 2) but inferred from mass balance

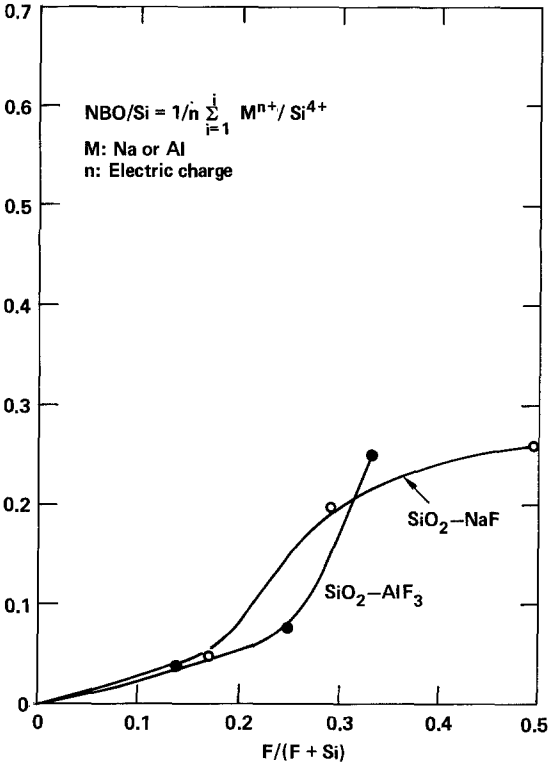

Fig. 8. Degree of polymerization (expressed as nonbridging oxygen per silicon, NBO/Si) of SiO_2-NaF and SiO_2-AlF_3 melts as a function of F/(F+Si) of the melts

and

$$18\,SiO_2+2\,AlF_3=3\,Si_4O_7F_2+Al_2(Si_2O_5)_3. \quad (3)$$

The justification for the formulations $Na_2Si_2O_5$, $Al_2(Si_2O_5)_3$ and $Si_4O_7F_2$ is given above. It is evident that fluorine acts as a depolymerizer of silicate melts and that the rate of increase in NBO/Si of the melts, expressed as a function of added F/(F+Si), is approximately equal whether the fluorine is added as AlF_3 or as NaF (Fig. 8).

The equilibrium constants for reactions (2) and (3) are

$$K_1=[Si_4O_7F_2]\ [Na_2Si_2O_5]/[SiO_2]^6[NaF]^2 \quad (4)$$

and

$$K_2 = [Si_4O_7F_2]^3[Al_2(Si_2O_5)_3]/[SiO_2]^{18}[AlF_3]^2. \quad (5)$$

In these expressions the AlF_3 and NaF notations are schematic expressions employed to obtain local neutrality around the F^- anions that are not a part of the fluorinated silicate network. The Raman spectra do not reveal the exact nature of these complexes, and the notations are used here only for stoichiometric purposes. By substituting mole fractions for activities, the value of K_1 may be calculated from the data in Table 3. At the temperature from which all melts were quenched (1,550° C), the value of K_1 does not depend on the proportion of the individual structural units, and the standard-state free energy of the reaction also remains constant (~ -15 kcal/mole).

The Raman spectroscopic data are insufficiently sensitive for calculation of the value of K_2 because, within experimental uncertainty, only $Si_4O_7F_2$ units can be detected. At given F/(F+Si) the abundance of $Si_4O_7F_2$ units in SiO_2-AlF_3 quenched melts is significantly greater than in SiO_2-NaF melts. As a result, $[Si_4O_7F_2]$ in equation (5) is greater than in equation (4). The spectra do show, however, a very significant proportion of SiO_2 units left, even with F/(F+Si)=0.33. In principle, there should, therefore, also be some aluminum fluoride in the melts. It is likely, however, that because $[Si_4O_7F_2](SiO_2-AlF_3)$ is greater than $[Si_4O_7F_2](SiO_2-NaF)$, and this activity term is raised to the third power in equation (5), K_2 is much greater than K_1. Consequently, the relative stability of sodium fluoride complexes in silicate melts greatly exceeds that of aluminum fluoride complexes. One may speculate, therefore, that in sodium aluminosilicate melts, a significantly greater proportion of the fluorine will occur associated with sodium rather than as aluminum fluoride complexes. Solution of fluorine in aluminosilicate melts is therefore likely to result in the stabilization of metal fluoride complexes (e.g., NaF type), and fluorine in exchange for bridging oxygen in the silicate network. This mechanism also leads to the formation of nonbridging oxygen in the melt. It is suggested that this mechanism may help explain the changes in physical and chemical properties of fluorine-bearing silicate melts compared with the fluorine-free analogues.

Acknowledgments. Critical reviews by Drs. P. Richet and H.S. Yoder, Jr., are appreciated.

References

Brawer SA, White WB (1975) Raman spectroscopic investigation of the structure of silicate glasses. I. The binary silicate glasses. J Chem Phys 63:2421–2432

Danckwerth P (1981) Phase relations in the system $Na_2O-Al_2O_3-SiO_2-H_2O-HF$ at 15 kbar. Carnegie Inst Washington Yearb 80:350–352

Davidon WC (1966) Variable metric method for minimization. ANL 5990, Argonne National Laboratory

Dumas P, Corset J, Carvalho W, Levy Y, Neuman Y (1982) Fluorine-doped vitreous silicate analysis of fiber optics preforms by vibrational spectroscopy. J Non-Cryst Solids 47:239–242

Fletcher R, Powell MJD (1963) A rapidly converging descent method for minimization. Computer J 6:163–168

Furukawa T, Fox KE, White WB (1981) Raman spectroscopic investigation of the structure of silicate glasses. III. Raman intensities and the structural units in sodium silicate glasses. J Chem Phys 75:3226–3237

Gilbert B, Mamantov G, Begun GM (1975) Raman spectra of aluminum containing melts and the ionic equilibrium in molten cryolite type mixtures. J Chem Phys 62:950–955

Hariyama C, Camp FE (1969) The effect of fluorine and chlorine substitution and fining of soda-lime and potassium-barium silicate glass. Glass Technol 10:123–127

Hartwig CM (1977) The radiation-induced formation of hydrogen and deuterium compounds in silica as observed by Raman scattering. J Chem Phys 66:227–239

Kogarko LN, Kriegman LD (1973) Structural position of fluorine in silicate melts (according to melting curves). Geochem Int 9:34–40

Kovalenko NI (1978) The reactions between granite and aqueous hydrofluoric acid in relation to the origin of fluorine-bearing granites. Geochem Int 14:108–118

Kozakevitch P (1954) Sur la viscosite des laitiers de hauts fourneaux. Rev Metall 51:569–587

Long DA (1977) Raman spectroscopy. McGraw-Hill, New York

Manning DAC (1981) The effect of fluorine on liquidus phase relationships in the system Qz–Ab–Or with excess water at 1 kb. Contrib Mineral Petrol 76:206–215

Matson JF, Sharma SK, Philpotts JA (1983) The structure of high-silica alkali-silicate glasses – a Raman spectroscopic study. J Non-Cryst Solids 58:323–352

McMillan P, Piriou B, Navrotsky A (1982) A Raman spectroscopic study of glasses along the joins silica-calcium aluminate, silica-sodium aluminate and silica-potassium aluminate. Geochim Cosmochim Acta 46:2021–2037

Mysen BO, Virgo D, Scarfe CM (1980) Relations between the anionic structure and viscosity of silicate melts – a Raman spectroscopic study. Am Mineral 65:690–711

Mysen BO, Finger LW, Seifert FA, Virgo D (1982a) Curve-fitting of Raman spectra of amorphous materials. Am Mineral 67:686–696

Mysen BO, Virgo D, Seifert FA (1982b) The structure of silicate melts: implications for chemical and physical properties of natural magma. Rev Geophys 20:353–383

Phillips JC (1984) Microscopic origin of anomalously narrow Raman lines in network glasses. J Non-Cryst Solids 63:347–355

Powell MJD (1964a) An efficient method for finding a minimum of a function of several variables without calculating derivatives. Computer J 7:155–162

Powell MJD (1964b) A method for minimizing a sum of non-linear functions without calculating derivatives. Computer J 7:303–307

Rabinovitch EM (1983) On the structural role of fluorine in glass. Phys Chem Glasses 24:54–56

Seifert FA, Mysen BO, Virgo D (1981) Quantitative determination of proportions of anionic units in silicate melts. Carnegie Inst Washington Yearb 80:301–302

Seifert FA, Mysen BO, Virgo D (1982) Three-dimensional network melt structure in the systems $SiO_2-NaAlO_2$, $SiO_2-CaAl_2O_4$ and $SiO_2-MgAl_2O_4$. Am Mineral 67:696–718

Seifert FA, Mysen BO, Virgo D (1983) Raman study of densified vitreous silica. Phys Chem Glasses 24:141–145

Shinozaki N, Okusi H, Mizoguchi K, Suginohara Y (1977) Electrical conductivity and IR spectra of Na_2O-SiO_2-NaF melts. Japan Inst Metall J 41:607–612

Takusagawa N (1980) Infrared absorption spectra and structure of fluorine-containing alkali silicate glasses. J Non-Cryst Solids 42:35–40

Walrafen GE (1967) Raman spectral studies of the effects of temperature on water structure. J Chem Phys 54:114–126

Wyllie PJ, Tuttle OF (1961) Experimental investigation of silicates containing two volatile components. II. The effects of NH_3 and HF in addition to water on the melting temperatures of granite and albite. Am J Sci 259:128–143

Yamamoto K, Nakashini T, Kasahara H, Abe K (1983) Raman scattering of SiF_4 molecules in amorphous, fluorinated silicon. J Non-Cryst Solids 59 and 60:213–216

Received October 1, 1984